Centrifugo-Magnetophoretic Purification of CD4+ Cells from Whole Blood Toward Future HIV/AIDS Point-of-Care Applications

Macdara Glynn[1], Daniel Kirby[1], Danielle Chung[1], David J. Kinahan[1], Gregor Kijanka[1], and Jens Ducrée[1]

Abstract

In medical diagnostics, detection of cells exhibiting specific phenotypes constitutes a paramount challenge. Detection technology must ensure efficient isolation of (often rare) targets while eliminating nontarget background cells. Technologies exist for such investigations, but many require high levels of expertise, expense, and multistep protocols. Increasing automation, miniaturization, and availability of such technologies is an aim of microfluidic lab-on-a-chip strategies. To this end, we present an integrated, dual-force cellular separation strategy using centrifugo-magnetophoresis. Whole blood spiked with target cells is incubated with (super-)paramagnetic microparticles that specifically bind phenotypic markers on target cells. Under rotation, all cells sediment into a chamber located opposite a co-rotating magnet. Unbound cells follow the radial vector, but under the additional attraction of the lateral magnetic field, bead-bound target cells are deflected to a designated reservoir. This multiforce separation is continuous and low loss. We demonstrate separation efficiently up to 92% for cells expressing the HIV/AIDS relevant epitope (CD4) from whole blood. Such highly selective separation systems may be deployed for accurate diagnostic cell isolations from biological samples such as blood. Furthermore, this high efficiency is delivered in a cheap and simple device, thus making it an attractive option for future deployment in resource-limited settings.

Introduction

Isolation and enumeration of specific cellular subtypes from a variety of medically relevant fluids is a core requirement in many medical diagnosis and clinical monitoring environments. The reduction in number of particular cells in the blood of a patient can be diagnostic of a number of diseases such as acquired immunodeficiency syndrome (AIDS) and hairy cell leukemia.[1,2] Conversely, the appearance or elevation of certain cells may indicate progression of diseases; for example, there is currently intensive research and commercial interest in the detection and enumeration of circulating tumor cells in blood samples.[3] Current technologies for such specific cellular monitoring (such as flow cytometry) are often large, expensive, and require highly trained personnel to operate. Alternatively, some bench-based kits are available that minimize the use of capital equipment by applying protocols such as chemical lysing and microscopy to the detection strategy. These kit protocols are often labor intensive with a number of points where operator intervention is required.

Lab-on-a-chip (LOC) strategies present an attractive option for reducing the costs, expertise, and labor time for the simplification of cellular monitoring devices in medical fields,[4] and there is a growing number of companies with commercialized instruments either on the market or in the

[1]Biomedical Diagnostics Institute, National Centre for Sensor Research, School of Physical Sciences, Dublin City University, Ireland

Corresponding Author:
Jens Ducrée, Biomedical Diagnostics Institute, National Centre for Sensor Research, School of Physical Sciences, Dublin City University, Glasnevin, Dublin, 9, Ireland.
Email: jens.ducree@dcu.ie

final stages of testing that are using these technologies for cell monitoring.[5,6] Such strategies shift the focus of a technology from highly expensive machinery with simple consumables to a small and low-cost detection device using highly engineered but cheaply manufactured consumables.[5] These devices often require operator intervention simply to add a sample to the diagnostic cartridge and insert the cartridge into an instrument. Fully automated fluid handling and other functions are then carried out within the system. Instead of a major investment in capital machinery that may overshoot the intended purpose, the LOC option places such diagnostics within the price range of most facilities, with minimal cost of ownership mainly constituted by the consumables (i.e., microfluidic chips). In addition, such instruments and chips are very specific in their purpose and so eliminate increased costs associated with unnecessary functionality that is often associated with capital equipment. A prime goal of developing such LOC strategies is to adapt the technology into point-of-care (POC) devices enabling deployment of cell-based medical monitoring to the site of high patient density, rather than shipping patient samples to (often remote) central laboratories. Deployment of POC devices has already been shown to positively influence the retention of patients in disease-monitoring programs in resource-poor settings.[7] The application of LOC and automation to HIV/AIDS POC diagnostics in resource-poor regions is a model for the validity of matching a particular technology to a specifically relevant societal need. HIV diagnostic devices employing LOC strategies have seen medical and commercial success since 2009 and have been extensively reviewed recently.[8,9]

A number of research groups have developed LOC techniques and devices enabling the purification of specific phenotypes from biological backgrounds. Many of these devices have made use of paramagnetic beads to bind cells in a mobile phase and subsequently relocate them to detectors or areas on a chip where they can be manually enumerated.[10–13] Often, the passage of sample in these devices has been driven by capillary flow. In the work presented here, we build on previous work carried out in this group in which the LOC strategy is integrated into a spinning platform, allowing rapid movement of sample through microfluidic structures and an increase in throughput by placing a number of such structures on a single, DVD-sized disc. This is the so-called "lab-on-a-disc" strategy.[14,15]

In an endeavor to develop a compact, user-friendly, and cost-efficient sample-to-answer device for highly accurate target cell counts, we introduce here a novel method for centrifugo-magnetophoretic cell separation that is amenable to complete integration into a lab-on-a-disc platform.[14,16] As a proof-of-concept and an intermediate step, this work implements a bead-based immunomagnetic isolation of cells expressing the CD4 antigen on the cell surface—CD4-expressing cells being the primary host cell of the HIV virus

and hence of prime diagnostic relevance. This work aims to demonstrate efficiency of cell capture as well as recovery of CD4-positive cells spiked into a fresh blood sample extracted via finger-prick lancets. Our separation is based on a recently developed centrifugo-magnetic platform for bead-based assays, which showed a 96% separation efficiency of biomimetic magnetic beads from a background of thousands of particles.[17] Although other multiforce centrifugal strategies have been used to separate cells (such as centrifugal forces combined with a dielectrophoretic force[18]), here we use a centrifugal force combined with a magnetic force that can be integrated onto the disk at very low cost, and additionally we target a specific cellular phenotype for isolation.

Operational Principle

Centrifugo-magnetic particle separation (**Fig. 1**) has so far been demonstrated using polystyrene beads in a magnetic field created by three co-rotating magnets (M1 to M3).[17] For the cell separations presented in this article, the outer magnets at positions M1 and M3 were removed, as it was found that a single magnet at M2 was optimum for the purpose of separating magnetically tagged CD4 cells from whole blood (**Figs. 1** and **2**). Samples are pipetted into the loading chamber (**Fig. 1ii**), and when the disc is spinning, cells and particles enter the focusing channel, where they are aligned along the wall distant to the magnet. Upon leaving the focusing channel, nonmagnetic particles (i.e., blood and/or spiked cells that do not bind to magnetic beads) sediment on straight, radial trajectories through the separation chamber directly into capture finger B, which is most distant from the magnet (referred to in the text as the "waste" chamber). In contrast, unbound magnetic beads are strongly deflected toward the permanent magnet located near the sidewall of the separation chamber at the M2 position. Finally, the subpopulation of magnetically tagged CD4 target cells that display a large magnetic moment and experience a large centrifugal force travel on an intermediate, moderately curved trajectory to capture area C, referred to in the text as the "capture" chamber (**Fig. 1**). On completion of a successful experiment, there are hence three destination regions in the structure. Position A is occupied by unbound excess magnetic beads. Position B ("waste") is populated by a mixed population of background material and nonselected spiked cells, for example, blood and/or HeLa cells in the current experiments. This mixed population will be depleted of the particular cell type to which the experimental magnetic beads are bound. Position C ("capture") will then be the locus to which the cells depleted from position B will be resolved. This means that the cells of interest will be positively selected and ultimately directed to the capture chamber, leaving a depleted mix of background material in the waste chamber.
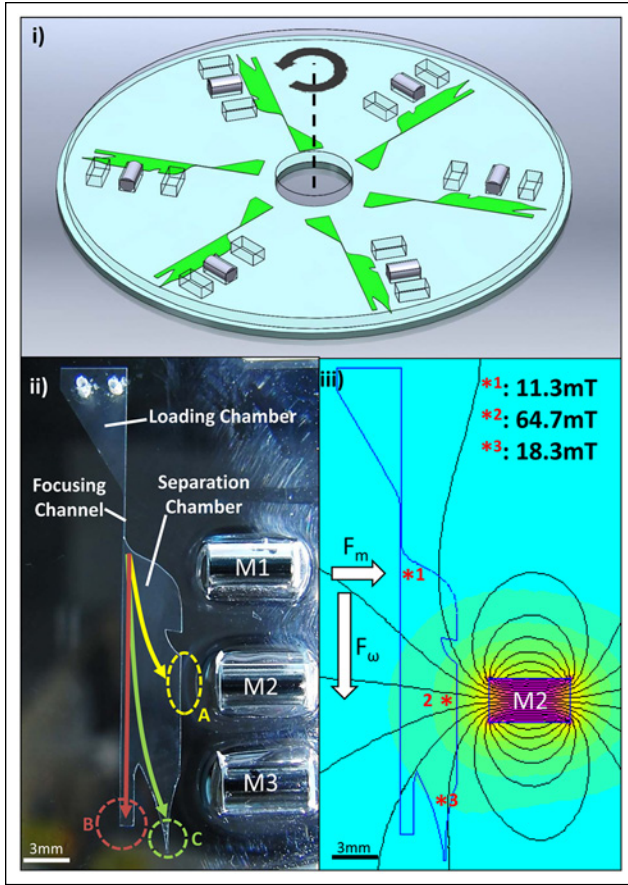
Figure 1. (**i**) Three-dimensional (3D) rendering of the lab-on-a-disc. The disc consists of a bottom layer of PMMA and a top layer of polydimethylsiloxane containing the microfluidic channels (green) and the co-rotating magnets (gray). For the experiments described, magnets were installed in only the M2 positions. The center of rotation is indicated by a dashed line, and the direction of rotation is indicated by an arrow. The depth of the chambers is 100 µm, and the width of the focusing chamber is also 100 µm. (**ii**) Photograph of one of the six on-disc microfluidic chambers with relevant features labeled: A, site of unbound bead collection; B, chamber for collection of undeflected, i.e., nonmagnetically tagged cells ("waste" chamber); C, chamber for collection of deflected, i.e., magnetic bead-bound cells ("capture" chamber). In the work presented here, the permanent magnets at M1 and M3 have been removed. (**iii**) Schematic of same chamber with magnetic field lines generated only by M2. Estimated strength of the magnetic field indicated at points (*1–3). Centrifugal force indicated by the arrow marked F_{ω}, and magnetic force indicated with the arrow marked F_m.

A key aspect of the separation performance mentioned here is the stopped-flow or batch mode characteristic (i.e., as in a regular centrifuge); there is no flow of liquid in the rotating system. Therefore, particles (i.e., cells or magnetic beads) will merely sediment through the residual priming medium in the chamber (in the disc frame). This is in contrast to common microfluidic systems in which liquid flow conveys the suspended particles by virtue of the Stokes drag.[19–21] These flow-based systems exhibit parabolic flow profiles and are prone to hydrodynamic instabilities and divergent flow around objects. By using a stopped-flow scheme, cells and particles in our structure will experience only the centrifugal and magnetic forces, as well as the velocity-dependent Stokes drag of the surrounding medium. This results in the sample acting as a collection of individual particles (i.e., blood cells) rather than a fluid. This strategy is integral to extracting the target particles of interest.

The separation of intrinsically nonmagnetic target cells from a mixed background population using magnetic beads is quite complex as the extent of deflection depends on the individual load of the attached magnetic tags. The amount of binding is, for instance, governed by the concentration of the magnetic beads, the amount of receptors expressed on the cell surface, the buffer composition, and the bead/sample incubation procedure.

Modeling of Particle Trajectories

To acquire an understanding of how the various particles in this system would behave and what forces would be necessary to achieve the best separation, theoretical calculations were carried out.

The particle trajectories are governed by the centrifugal force

$$\left| F_{\omega} \right| = m\, r\, \omega^2,\tag{1}$$

where m is the particle mass, r is the radial distance from the center of rotation, and ω^2 is the angular frequency of rotation. The magnetic force is given by

$$\left| F_M \right| = \frac{\left| \chi_P - \chi_M \right| \cdot V_P}{\mu_0} \left| (\vec{B} \cdot \nabla)\vec{B} \right|,\tag{2}$$

where χ_P and χ_M are the magnetic susceptibilities of the particle and the medium, respectively, V_P is the volume of the particle, μ_0 is the magnetic permeability of the liquid, and B is the local magnetic field strength. The Stokes drag follows the equation

$$\left| F_D \right| = 6\pi\, \eta\, R_0\, v,\tag{3}$$

where η is the viscosity of the liquid, R_0 is the radius, and v is the velocity of the particle.

Unbound cells (i.e., red blood cells) will experience only the radial centrifugal force and the frictional Stokes drag pointing opposite to the direction of their migration through the stagnant liquid. All magnetic particles, whether unbound or attached to target cells, will, in addition, be exposed to the (local) magnetic force, which acts essentially perpendicular to the radial direction. Managing the balance of these three forces on each of the three particle species in
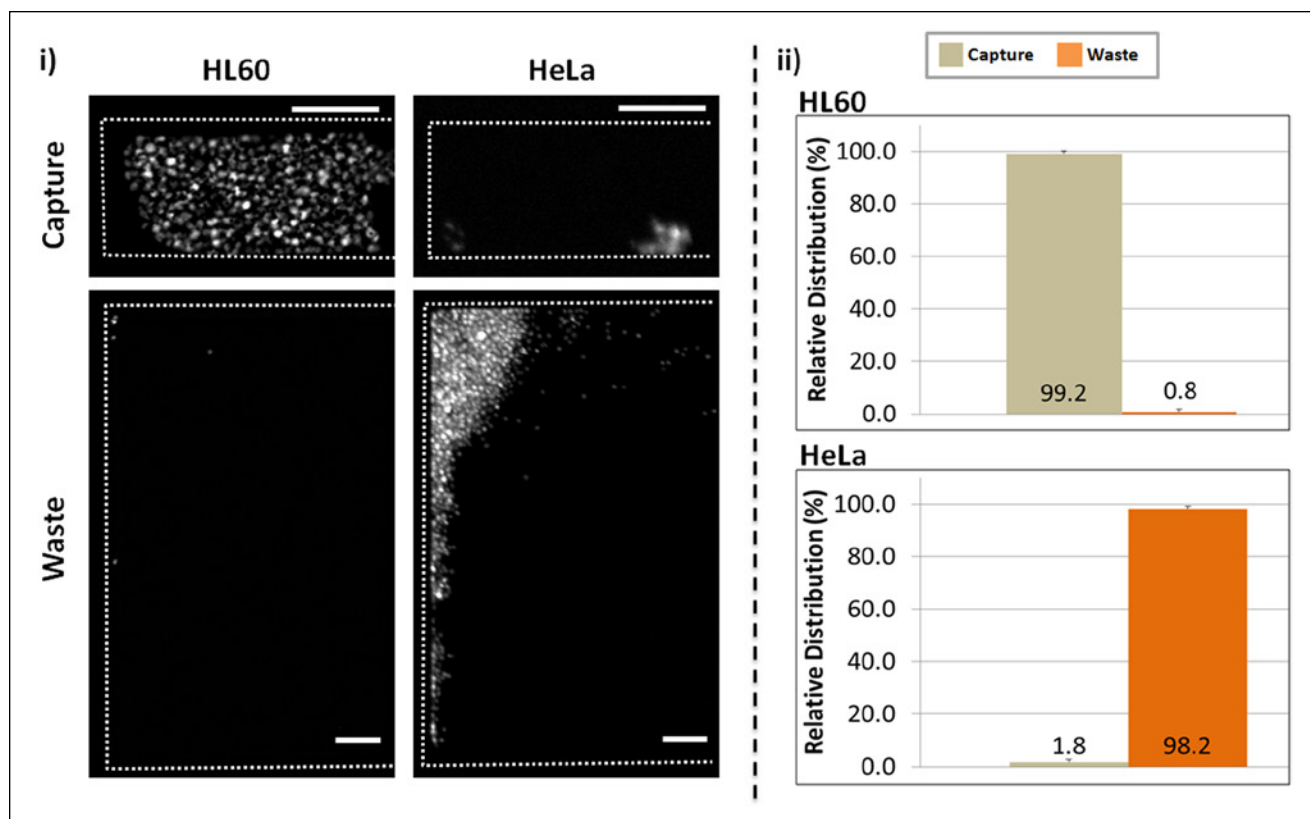
Figure 2. Centrifugo-magnetophoretic distribution of homogenous, i.e., single-phenotype, cultured human cell populations. (**i**) Fluorescent images of either HL60 (left) or HeLa (right) cells imaged following centrifugo-magnetophoresis with optimized spin speeds and time. White dashed lines represent edges of the chambers as seen in differential interference contrast (DIC). Scale bars are 100 μm. (Note scale difference between capture and waste chambers.) (**ii**) Bar charts were generated based on the RawIntDen values measured in both chambers and represent the relative distribution of fluorescence between capture and waste chambers. Error bars indicate one standard deviation.

question, mainly by means of the spinning frequency ω, the chamber geometry, and the alignment of the magnet(s), is pivotal to the sorting of tagged cells from such a complex background.

Another rotationally induced force, the Coriolis force, is notably smaller than the other forces. However, the Coriolis force may still affect the predominantly radial travel of nonmagnetic cells. The Coriolis force acts in the plane of the disc, perpendicular to the motion of the particle and opposite to the direction of rotation. Therefore, the direction of rotation was chosen to ensure the Coriolis force acts to drive the nonmagnetic (background) cells away from the magnets and help focus the flow of these cells into a narrow stream against the wall of the chamber.

Materials and Methods

Disc Fabrication and Priming

The microfluidic discs used in this system were formed from a silicone elastomer; polydimethylsiloxane (PDMS;

Dow Corning, MI) mixed at a ratio of 5:1 base and curing agent. The procedure for making a master has been described in detail elsewhere.[17,22] As the cavities for securing the co-rotating magnets in the PDMS were too large to be formed by the lithography master (5 mm in height), a polymer mold was printed on an uPrint SE 3D printer (Stratasys, MN). This mold consisted of a large, disclike structure with appropriately sized posts descending to the silicone base. The mold was held in place during the PDMS curing process by guide pins. These pins also allowed alignment of the mold to be reproduced for multiple discs. When the PDMS was poured, it formed both the lithographic structures of the microchannels and also the large cavities for the magnets.

Once the magnet-positioning mold was aligned above the silicon master, 26 g of PDMS was poured into the mold and cured in an oven at 70 °C for 40 min. The PDMS was cut out and pealed from the wafer, leaving the microfluidic structures on the underside and cavities for placing the magnets through the PDMS. Sample-loading holes and vents were defined in the PDMS at appropriate locations using a

dot punch. Finally, the PDMS was mounted to a PMMA base. This has been described previously.[17] Both the depth of the chamber and the width of the focusing channel on the fully assembled disc measured 100 μm.

To prime the microchannels and structures, the disc was placed under vacuum for at least 1 h, following which a large drop of priming buffer (phosphate-buffered saline [PBS] pH 7.4, 0.1% w/v bovine serum albumin [BSA], 1 mM EDTA) was immediately placed on the surface of the PDMS, covering both the sample ports of the loading chamber. Degas driven flow then primes the channels.[23] Magnets used were NdFeB N45 cylindrical magnets, with a diameter of 3 mm and a height of 6 mm (Supermagnete, Germany). Magnets were placed in the molded cavities before the samples were loaded to the disc.

The stopped-flow characteristic arises from priming the dead-end chamber to its maximum volume capacity. In a second step, a sample volume is introduced to the chamber by displacing the same volume of priming buffer out of the second port into the sample input region.

The magnetic field strength in the centrifugo-magnetophoretic chamber was estimated using the finite element method magnetics software package (FEMM v4.2).[24]

Blood Extraction and Cell Culture

Blood was extracted directly from healthy donors via finger prick using 1.5 mm sterile lancets (BD Biosciences, Franklin Lakes, NJ). To prevent coagulation of the blood sample, 60 mM EDTA solution was immediately added to the sample to result in a final concentration of 6 mM EDTA in the whole blood. The whole blood/EDTA sample was then further diluted 1:3 in blood dilution buffer (100 mM PBS, pH 7.4, 0.05 mM EDTA). Blood was isolated and prepared fresh, directly before experimental use.

Where indicated, white blood cells (WBCs) were extracted from whole blood using standard-density gradient separation with Ficoll-Paque 1077 (Sigma-Aldrich, St. Louis, MO). Briefly, extracted blood was diluted 1:3 in blood dilution buffer and carefully layered over Ficoll-Paque in a 15 mL conical tube. Following a 300g, 15-min spin in a swing-out bucket centrifuge (Hettich Zentrifugen, Germany), the WBC-containing "buffy coat" layer was isolated and resuspended in blood dilution buffer. When appropriate, cultured cells were spiked into whole blood or WBC samples as indicated.

All cell culture reagents were obtained from Sigma-Aldrich unless otherwise stated. HeLa and HL60 cells (both from DSMZ, Braunschweig, Germany) were cultured in 75 cm^2 flasks in DMEM or RPMI 1640 media, respectively, with 10% uninactivated fetal bovine serum, 100 U/mL penicillin, and 100 μg/mL streptomycin. Cultures were maintained at 37 °C with 5% CO_2. Harvesting of HeLa cells was carried out by incubation in 5 mL 0.25% trypsin/0.1% EDTA at 37 °C for 5 min followed by neutralization with 5 mL DMEM culture medium. Cells were centrifuged at 300g for 4 min and resuspended in DMEM culture media. HL60 cells were harvested by removing a volume of culture, centrifuging as above, and resuspension in RPMI 1640 culture media.

Where indicated, live cells were fluorescently stained with either NucBlue Live Cell Stain or 5nM Syto64 (both from Life Technologies, Carlsbad, CA) according to the manufacturer's instructions.

Dynabead CD4 Sample Incubation

Experimental samples composed of homogenous cell cultures (HeLa or HL60), mixed cell cultures (HeLa and HL60), or blood spiked with either homogenous or mixed cultures were treated with Dynabeads CD4 magnetic beads (Life Technologies). Incubations were carried out in a 2 mL Eppendorf tube, and final incubation volume was 200 μL per sample, composed of 140 μL incubation buffer (PBS pH 7.4, 0.1% w/v BSA, 1 mM EDTA), 50 μL experimental sample, and 10 μL Dynabead CD4. In the sample as described, the beads are present at a final concentration of about 1×10^4 μl^{-1}. A double layer of Parafilm (Pechiney Plastic Packaging Company, Chicago, IL) was placed between the cap and the tube, and incubation was performed at room temperature with rotation for 10 min. Three microliters of Dynabead CD4–treated sample was introduced to the loading chamber of the disc via pipetting. Where indicated, the incubation time was reduced.

Discs were spun on a custom-built test stand composed of a Cool Muscle CM2-X-56B10A motor (Muscle Corp, Osaka, Japan) with a custom chuck that was machined for securely attaching standard discs to the servo-motor shaft. A desktop PC (Dell, Round Rock, TX) was used to control the spin-speed of the motor.

Microscopic Imaging and Quantification of Signal

Following spin cycles on the test stands, fluorescently stained cells were visualized on disc using an Olympus IX81 inverted epifluorescent microscope (Olympus, Tokyo, Japan). Because of similar excitation and emission fluorescence profiles, NucBlue- and Syto64-stained cells were visualized using a DAPI or TexasRed filter set, respectively. Unstained cells were visualized using differential interference contrast (DIC) on the same microscope. Relative distribution of fluorescent signal between the waste (B) and capture (C) structures of the disc were calculated as follows using the ImageJ software package (National Institutes of Health, Bethesda, MD).[25] For a given experiment, the overall cell coverage was observed in both the capture and waste, and the chamber containing the largest zone of cell-occupied area was selected. A region of interest (ROI) was
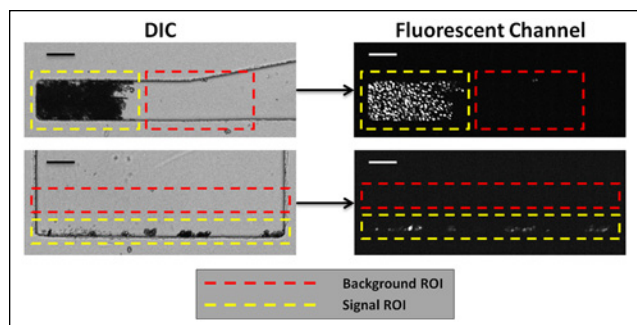
Figure 3. Calculation of relative distribution of fluorescence between capture and waste chambers. Differential interference contrast images of the capture chamber were used to draw a signal region of interest (ROI) encompassing the cell/bead occupied area in the chamber (yellow hatched box). An identical background ROI was then placed on a non–cell/bead occupied area of the same chamber to measure the level of background fluorescent signal in the chamber (red hatched box). The area of the signal ROI was calculated, and both signal and background ROIs with identical area were drawn on the waste chamber, encompassing the cell/bead occupied and nonoccupied areas, respectively. All ROIs were then applied to the fluorescent images, and RawIntDen values were measured. The values of the background ROIs were subtracted from the relevant signal ROI for each chamber. Note: In the shown example, the cell/bead occupied area of the capture chamber was observed to be the larger of the two chambers and hence the benchmark for appropriate ROI size. Scale bars are 100 μm.

generated using a DIC image that encompassed all cells present in the selected chamber, and the area of this ROI was calculated. A second ROI was then generated on the partner chamber and was reshaped to encompass the chamber itself with minimal coverage of the surrounding PDMS. Importantly, this second ROI was given dimensions to result in identical overall area to the first ROI. These ROIs were then applied to the corresponding fluorescent images for each chamber, and the raw integrated density values ("RawIntDen" measurement in ImageJ) of the ROIs were measured. RawIntDen values were also measured in identically sized and shaped ROIs placed on cell-free regions of the chambers to generate background signal values, which were subtracted from the values generated from the cell-containing ROIs (**Fig. 3**).

Relative distribution of fluorescent signal was then calculated using the following:

$$\left(\frac{Waste\ RawIntDen + Capture\ RawIntDen}{100} \right)$$
$$\times Waste\ RawIntDen = \textbf{\textit{Relative Waste Signal}}.$$

$$\left(\frac{Waste\ RawIntDen + Capture\ RawIntDen}{100} \right)$$
$$\times Capture\ RawIntDen = \textbf{\textit{Relative Capture Signal}}.$$
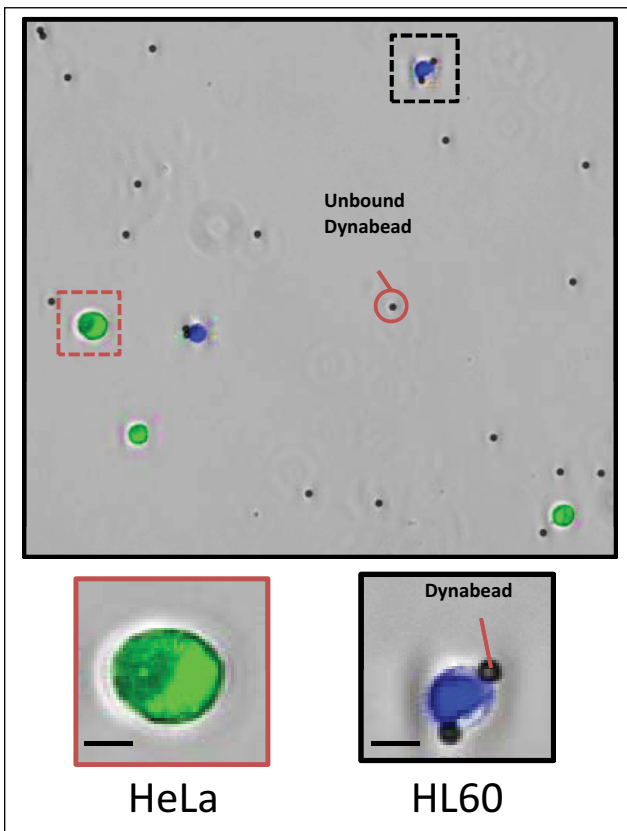
Figure 4. Specificity of Dynabead CD4. Fluorescence image of HL60 (blue, CD4 positive) and HeLa (green, CD4 negative) following incubation of a mixed sample with Dynabeads CD4 magnetic beads. Scale bars are 10 μm.

Experimental Results

Specificity of Dynabead CD4 Magnetic Bead Binding

The specificity of the Dynabeads CD4 reagent was first demonstrated within our particular experimental conditions. Both HL60 (CD4 positive) and HeLa (CD4 negative) cells were independently stained with NucBlue and Syto64, respectively. Equal numbers of each cell type (1×10^5 ml^{-1}) were then mixed and incubated with the Dynabead CD4 reagent as described above. An 8 μL aliquot of the incubated sample was deposited on a microscope slide and a coverslip placed on top of the sample. Cells were imaged as described. A blue color was applied to fluorescence detected in the DAPI channel, and a green color was applied to fluorescence detected in the TexasRed channel; ImageJ was then used to merge the channels into a single image.

In all fields that were viewed, the Dynabeads were found co-localizing only with HL60 (colored blue in **Fig. 4**) and never with HeLa (colored green in Fig. 4), thus demonstrating a high binding specificity of the Dynabeads for CD4

positive cells under the experimental conditions used throughout this work. Furthermore, the average number of Dynabeads binding to a single HL60 cell was about 4 (data not shown).

Centrifugo-magnetophoretic Routing of Homogenous Cell Populations

To calibrate the settings of the spin stand to achieve the optimal balance between magnetic and radial forces that segregate CD4-positive cells to the capture chamber while ensuring that CD4-negative cells maintain their trajectory along the radial axis to the waste chamber, initial experiments were performed using homogenous cultures of either CD4-positive HL60 or CD4-negative HeLa cells. Equal numbers of cells from each cell line (1×10^6 ml^{-1}) were independently stained with NucBlue, incubated with the Dynabead CD4 reagent, and processed by centrifugo-magnetophoresis as described. As neither the strength nor the position of the permanent magnet is adjustable on the disc, the variable factor that can be controlled to achieve optimal magnetic/radial force balance is the rotor speed. It is also possible to adjust this balance by altering the viscosity of the priming buffer or the size of the magnetic beads; however, for the current experiments, only the rotor speed was examined as this can be rapidly adjusted in real time along the experiment. Following completion of the spin cycle, the disc was visualized on an IX81 Olympus epifluorescent microscope. Images were taken at the capture, waste, and M2 positions for all experiments, and relative distribution of fluorescence was calculated as described.

The optimal spin speed for the centrifugo-magnetophoretic disc to segregate the homogenous cells to the distributions shown in **Figure 2** was found to be 10 Hz (RCF = 18 × g). At this speed, the discs were spun for 40 min to allow the majority of the sample to exit the loading chamber and progress to the capture and/or waste chambers. In most cases, a small percentage of the experimental sample would remain in the loading chamber, and increased centrifugal force or time would not promote these cells into the segregation chamber. These "stalled" cells may result from their binding to the PDMS in the chamber. A BSA concentration of 0.1% in the priming solution minimized the proportion of such stalled cells. Although at slower spin speeds (about 5–7 Hz) the efficiency of capture was not adversely affected, the time required to resolve the cells to their relevant chambers increased to 60 min, and a number of the target cells were captured at the M2 magnetic position rather than the capture chamber. This is due to the increased relative magnetic force relative to the centrifugal force. Conversely, with spin speeds in excess of 12 Hz, an increasing number of target cells resolved to the waste chamber, as the radial force was increased sufficiently to overcome the lateral magnetic force and hence prevent a number of cells from

Table 1. Summary of fluorescence distributions with reduced off-disc incubation times.

	Reduced Cell/Bead Off-Disc Incubation Time (% Fluorescence Distribution)		
	10 min	1 min	0 min
Capture	99.2 ± 1.1	94.9 ± 3.7	89.1 ± 2.7
Waste	0.8 ± 1.1	5.1 ± 3.7	10.9 ± 2.7

deflecting from the radial trajectory. The final combination of 10 Hz for 40 min gave the most favorable combination of sensitivity (CD4-positive cells to capture), specificity (CD4-negative cells to waste), and time to completion.

Under the above-defined conditions, and using samples composed of homogenous cell cultures, the current structure achieved a balance between magnetic and radial centrifugal forces that efficiently directed >99% of HL60 cells to the capture chamber while guiding CD4-negative HeLa cells to the waste chamber. A small number of HL60 cells were guided to the waste chamber. This may be attributed to a lower efficiency of Dynabead binding to these cells during incubation, either due to steric hindrance from other cells or to a small subpopulation of HL60 cells expressing lower CD4 levels. Similarly, a small number of HeLa cells were directed to the capture chamber. Higher magnification of these cells did not show any visible co-localizing Dynabeads, suggesting this low level of nonspecific capture is not due to bead interaction but due to other factors such as cell-cell binding. In the case of both HL60 and HeLa, unbound Dynabeads were captured at the M2 position of the chamber. As expected, the area occupied by unbound beads in the HeLa experiments was larger than that observed in the HL60 experiments as the beads were not sequestered by cells.

The Dynabeads CD4 reagent used in these experiments can also be supplied as part of a kit (T4 Quant Kit, Life Technologies). This kit allows bench-based CD4 enumeration from a blood sample of a diagnostic quality but without the use of capital equipment other than standard laboratory apparatus (pipettes, disposable tubes, etc.) and a fluorescent microscope. The 10 min off-disc incubation step to mix cells with beads (see the "Materials and Methods" section) was selected as it is a required step when using the T4 Quant kit. However, as the experimental sample volume that will be exposed to magnetic isolation is significantly lower in the centrifugo-magnetophoresis strategy (3 μL compared with 425 μL), experiments reducing or eliminating the incubation step on the disc-based system were carried out on HL60 cells (**Table 1**).

When processed on a centrifugo-magnetophoresis system, the requirement for the incubation step is reduced. Although there is a downward trend as the incubation time

reduces, when it is eliminated entirely, about 90% of the target cells are still captured. In an advancement of the experiments shown in **Figure 2**, we demonstrated that when HL60 and HeLa cells are mixed into a heterogeneous population, the centrifugo-magnetophoresis system can separate the HL60 cells from the background HeLa with high efficiency (**Supplementary Information S1**).

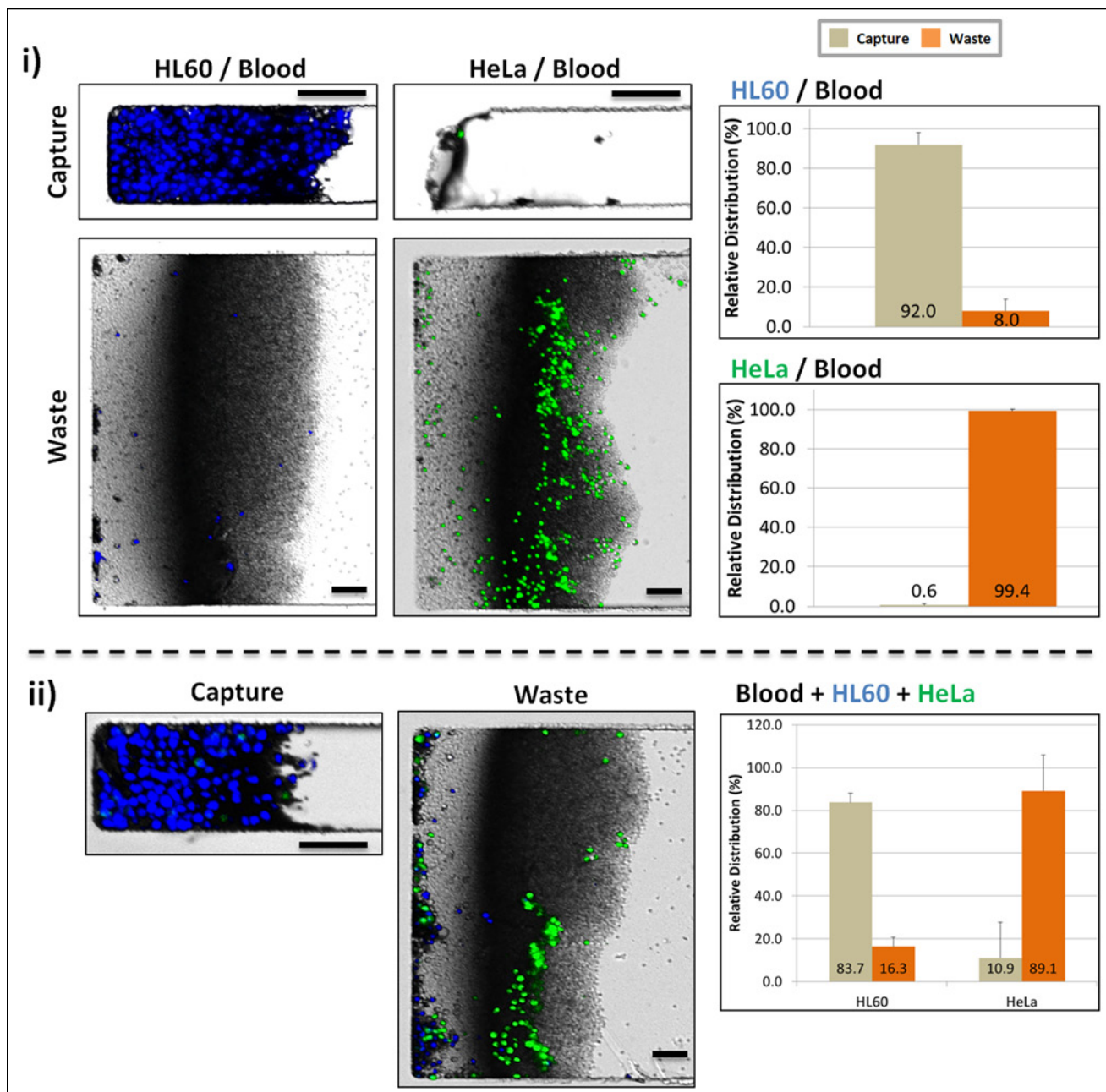## Centrifugo-magnetophoretic Isolation of CD4-Positive Cells from Blood

The ability to purify (or otherwise identify) cells of interest from a background of similar but interfering materials is of primary concern for cell detection technologies.[20,26,27] This is of particular importance in medical settings, where type I or type II errors (false-positive and false-negative, respectively) can lead to misdiagnosis of presenting patients, thus resulting in increased costs and patient distress due to unnecessary therapies or delayed initiation of treatment.[6] Although the previously introduced segregation of two cell lines with distinct phenotypes in buffer medium is of interest predominantly to the research community, the investigation of complex fluids such as whole blood is of paramount medical and commercial significance. Lab-on-a-disc strategies have been used in the isolation of macro-fractions of blood such as the hematocrit and plasma.[28–30] To further advance the disc strategy, demonstrating that specific cellular phenotypes can also be isolated from medically relevant backgrounds on these systems yet still maintain the amenability to low-cost manufacture and minimal complexity in an associated apparatus is an advantage of lab-on-a-disc and of interest to industrial developers.[5] To this end, we examined the ability of our system to isolate the CD4 cellular phenotype from a background of whole blood. To further validate the potential application of the current platform for cheap and robust medical diagnosis, operator-derived finger-prick capillary blood was used rather than intravenous blood, which must be extracted by a trained medical practitioner.

These experiments were examined in two stages. Initially, the efficiency of the system for isolating a homogenous, CD4-positive cell population from blood was investigated, followed by experiments in which dual staining was used to investigate the level of contaminating CD4-negative cells copurifying with the HL60 cells when isolated from the blood background. Whole blood was extracted from healthy donors and processed for anticoagulation as described. In the case of the homogenous cell experiments, stained HL60 or HeLa cultures were spiked to blood. For the mixed cell experiments, HL60 cells were stained with NucBlue, and HeLa cells were stained with Syto64. Cells were washed to prevent nonspecific staining, and then aliquots were spiked to the same blood sample, which was immediately followed by Dynabead CD4 incubation and

centrifugo-magnetophoresis at 10 Hz for 40 min. Cultured cells were spiked into the blood at a concentration of 1×10^5 ml^{-1}. ImageJ was used to merge the fluorescent channels with DIC into a single image.

Because of the significantly increased complexity of the matrix, the resolution was expected to fall short of the experiments using only cultured cells (**Fig. 2**; **Suppl. Fig. S1**). Yet the centrifugo-magnetophoretic lab-on-a-disc platform demonstrates an efficient isolation of target CD4-positive cells from a complex biological background sample. In the case in which a homogenous population was present in whole blood, more than 90% of HL60 cells were resolved to the capture chamber whereas the blood material resolved to the waste (**Fig. 5i**). In the parallel experiment, CD4-negative HeLa cells were resolved almost entirely to the waste chamber along with the blood, leaving the capture chamber essentially empty (**Fig. 5i**). Unbound Dynabeads were captured at the M2 position, with a larger mass of beads present in the experiments using CD4-negative cells (data not shown). When challenged with a dual population of spiked cells in the blood sample (representing two distinct cellular phenotypes), our separation system achieved >80% capture of the CD4-positive cells, whereas about 10% of the nontarget cells were co-isolated with the cells of interest. The lower efficiency of separation compared with the homogenous cell experiments may represent a phenomenon in which cell-cell interactions and immunocomplex formation may capture nontarget cells in macro-cellular complexes along with the positively selected population. Interestingly, the efficiency of HL60 capture is similar between **Supplemental Figure S1** (85.2%) and **Figure 5ii** (83.7%), experiments representing co-incubation of both phenotypes in the absence and presence of blood, respectively. This would suggest that the presence of blood did not have a notable effect on the efficiency of separation and that the reduction of separation efficiency for cell line experiments is merely an artifact related to cell culture. As the efficiency of HL60 isolation from blood in the absence of HeLa is higher (92.0%; **Fig. 5i**), this supports the notion that the reduction in efficiency is due to the cultured and spiked nature of the target cells and may not be representative of the native wild-type CD4 population in the blood. Further experiments focusing on the isolation of native CD4 T$_h$ cells from blood are ongoing.

To investigate whether the concentration of spiked cultured cells had an effect on the efficiency of the system, further experiments were carried out in which 5×10^4 ml^{-1} and 2×10^5 ml^{-1} HL60 cells were spiked to the blood. These represent 0.5× and 2× concentrations, respectively, of spiked cells relative to that shown in **Figure 5**. Isolation in these experiments showed efficiencies of 93.0% ± 1.4% and 94.0% ± 4.2%, respectively, indicating that (within the ranges tested) the concentration of spiked cells did not significantly alter the efficiency of isolation.

Figure 5. Centrifugo-magnetophoretic distribution of CD4-positive and/or CD4-negative cells from a whole blood background. (**i**) Whole capillary blood derived from finger-prick lancet extraction spiked with homogenous stained cultures of either HL60 (left) or HeLa (right) was processed by centrifugo-magnetophoresis. (**ii**) A heterogeneous sample of NucBlue stained HL60 and Syto64 stained HeLa cells was spiked into a single whole capillary blood sample and processed by centrifugo-magnetophoresis. In all images, HL60-derived fluorescence is assigned a blue color, and HeLa-derived fluorescence is assigned a green color for clarity. Differential interference contrast (DIC) microscopy was used to visualize the blood sample (seen in the waste chamber). The dark regions in the capture chamber seen in DIC represent the cell-bound beads, with some bead clusters that escaped capture at M2. Bar charts were generated based on the RawIntDen values measured in both chambers and represent the relative distribution of fluorescence between capture and waste chambers. Error bars indicate one standard deviation. Scale bars are 100 µm.

Many of the medically relevant cellular blood assays are concerned only with the WBC population in a sample, and parallel work carried out in the research group has focused on the applications of on-disc buffy coat extraction as a means of reducing the overall volume of a whole-blood sample that must run through the microfluidic structures of a POC device. To investigate if the current centrifugo-magnetophoretic lab-on-a-disc device will isolate cells of

Table 2. Summary of data from all experiments: homogenous cell population (% fluorescence distribution).

	HL60	HeLa	HL60/Blood	HeLa/Blood	HL60/Buffy Coat	HeLa/Buffy Coat
Capture	99.2 ± 1.1	1.8 ± 2.7	92.0 ± 5.9	0.6 ± 0.8	91.3 ± 6.0	7.8 ± 6.5
Waste	0.8 ± 1.1	98.2 ± 2.7	8.0 ± 5.9	99.4 ± 0.8	8.7 ± 6.0	92.2 ± 6.5

Table 3. Summary of data from all experiments: mixed cell populations (% fluorescence distribution).

	HL60/HeLa	HL60/HeLa/ Blood	HL60/HeLa/ Blood
Capture	85.2 ± 5.6	83.7 ± 4.3	10.9 ± 16.8
Waste	14.8 ± 5.6	16.3 ± 4.3	89.1 ± 16.8

interest from such a background sample, stained cells were spiked into a blood sample, and then a standard off-disc Ficoll-Paque buffy coat band extraction protocol was performed. The resulting sample (composed of native WBC and the spiked cells) was then incubated with Dynabead CD4, spun, and visualized as described above. Results of these experiments are included in **Table 2** and showed >90% efficient isolation of the spiked CD4-expressing HL60 cells, very similar to the results generated using whole blood. **Table 3** sums up the data pertaining to mixed cell populations from all experiments. Cell lines underlined represent the line in the experiment that was quantified.

Conclusions and Outlook

Coupled with molecular medicine, access to reliable and accurate cellular diagnosis technologies is rapidly becoming a major determinant of improving the prognosis of patients inflicted with various metabolic and infectious illnesses.[2,31–33] In the case of cellular diagnosis, the hardware and expert personnel required to deploy the technologies have been restrictive in delivering rapid sample-to-answer results to a patient; furthermore, the cost factor has largely limited the technology to high-income regions. Because of its inherent portability and relatively simple manufacture, the application of lab-on-a-chip technologies to cellular diagnostic applications has the potential to be a turning point in delivering affordable medical intervention to the bedside.[5] However, to be a viable option, the accuracy of such devices should be on a par with flow cytometry, the current gold standard in cellular analysis. Of critical importance to the development of such technology is the reliable on-chip isolation of relevant cells from a complex biological background. Previous work in our group has demonstrated the ability of a lab-on-a-disc centrifugo-magnetophoretic platform to efficiently separate a population of rather monodisperse magnetic beads from a background of other beads.[17] In our

work presented here, we for the first time demonstrated a significant advancement of this system leveraging highly efficient biological applications by enabling target cell isolation from a complex biological background based on specific cell-surface phenotypes. Furthermore, for cell isolation, the only hardware required is a speed-controlled spinning motor with a low-cost, reusable, on-disc magnet.

The system positively isolates a specific cellular phenotype of interest and deposits it to a reservoir that may be linked to structures that could further process the isolate to generate an on-disc indication of concentration. We used the system to specifically target and isolate cells expressing the HIV/AIDS-relevant CD4 epitope, a cell surface marker normally expressed on T-helper lymphocytes in whole blood. Based on the fluorescence distribution between the capture and waste structures of the chamber, the efficiency of the system consistently demonstrated >85% isolation of cells when samples of CD4-positive cells were mixed with a sample of background CD4-negative cells. When this cellular mix was placed into a sample of whole blood, the efficiency of CD4-positive isolation was essentially maintained, suggesting that medically relevant samples will not pose a further significant challenge to the ability of this system to successfully isolate cells of interest. Importantly, the experiments presented in this work used cultured human cells spiked into a blood sample to demonstrate the proficiency of the system. Such cells often tend to generate cell-to-cell interactions resulting in binding and clumping,[34] which in the case of the experiments shown here may have reduced the perceived efficiency of the system. Indeed, when CD4-positive cultured cells alone (i.e., CD4-negative HeLa cells were absent) were introduced into a blood sample and processed on the centrifugo-magnetophoretic system, the efficiency of purification was increased from 83.7% to 92.0%. We are hopeful that this is an indication that the efficiency of the system may be further increased when there are no spiked cultured cells present in a sample at all, and only native wild-type CD4 T-helper lymphocytes are targeted in the blood.

As the blood used in these experiments was isolated by a simple finger-prick extraction (similar to that performed at home by diabetes patients) rather than intravenous extraction without any visible clot formation or other identifiable caveat, these data suggest that the platform is robust enough to be adapted to use by minimally trained personnel. Such a user-friendly system, which lends itself to cost-efficient mass manufacture, would be attractive for the development

of a disposable diagnostic platform that identifies patients presenting particular cellular disease symptoms or to monitor the progression of an active treatment program. Indeed, developing a POC system for monitoring the concentration of native levels of CD4-positive cells in a blood sample is a prime societal and commercial target for current HIV/AIDS programs, particularly in resource-poor regions such as Sub-Saharan Africa.[35] Integrating the cell isolation system presented in this article with other emerging, on-disc cell-counting microfluidic strategies developed would represent a key advance in bringing high-end lab-on-a-disc–based cell-counting technology to the bedside.

Acknowledgment

Declaration of Conflicting Interests

Funding

References

1. World Health Organization. *Rapid Advice: Antiretroviral Therapy for HIV Infection in Adults and Adolescents*; World Health Organization: Geneva, Switzerland, 2009.

2. Cheson, B. D.; Bennett, J. M.; Grever, M.; et al. National Cancer Institute-Sponsored Working Group Guidelines for Chronic Lymphocytic Leukemia: Revised Guidelines for Diagnosis and Treatment. *Blood* **1996**, *87*, 4990–4997.

3. Pavlos, M.; Michael, K. Diagnostic Value of Circulating Tumor Cell Detection in Bladder and Urothelial Cancer: Systematic Review and Meta-analysis. *BMC Cancer* **2011**, *11*, 336–350.

4. Anderson, D.; Crowe, S.; Garcia, M. Point-of-Care Testing. *Curr. HIV/AIDS Rep*. **2011**, *8*, 31–37.

5. Chin, C. D.; Linder, V.; Sia, S. K. Commercialization of Microfluidic Point-of-Care Diagnostic Devices. *Lab Chip* **2012**, *12*, 2118–2134.

6. Murtagh, M. UNITAIDS Technical Report: HIV/AIDS Diagnostic Landscape. *HIV/AIDS Diagnostic Landscape*, May **2011**.

7. Jani, I. V.; Sitoe, N. E.; Alfai, E. R.; et al. Effect of Point-of-Care CD4 Cell Count Tests on Retention of Patients and Rates of Antiretroviral Therapy Initiation in Primary Health Clinics: An Observational Cohort Study. *Lancet* **2011**, *378*, 15721579.

8. Glynn, M. T.; Kinahan, D.; Ducree, J. CD4 Counting Technologies for HIV Therapy Monitoring in Resource-Poor Settings: State-of-the-Art and Emerging Microtechnologies. *Lab Chip* **2013**, *13*, 2731–2748.

9. Boyle, D. S.; Hawkins, K. R.; Steele, M. S.; et al. Emerging Technologies for Point-of-Care CD4 T-Lymphocyte Counting. *Trends Biotechnol*. **2012**, *30*, 45–54.

10. Furdui, V. I.; Harrison, D. J. Immunomagnetic T Cell Capture from Blood for PCR Analysis Using Microfluidic Systems. *Lab Chip* **2004**, *4*, 614–618.

11. Gao, D.; Li, H.; Guo, G.; et al. Magnetic Bead Based Immunoassay for Enumeration of CD4+ T Lymphocytes on a Microfluidic Device. *Talanta* **2010**, *82*, 528–533.

12. Ymeti, A.; Li, X.; Lunter, B.; et al. A Single Platform Image Cytometer for Resource-Poor Settings to Monitor Disease Progression in HIV Infection. *Cytometry Part A* **2007**, *71A*, 132–142.

13. Li, X.; Breukers, C.; Ymeti, A.; et al. CD4 and CD8 Enumeration for HIV Monitoring in Resource-Constrained Settings. *Cytometry B Clin. Cytom*. 2009, *76B*, 118–126.

14. Burger, R.; Ducrée, J. Handling and Analysis of Cells and Bioparticles on Centrifugal Microfluidic Platforms. *Expert Rev. Mol. Diagn*. **2012**, *12*, 407–421.

15. Burger, R.; Kirby, D.; Glynn, M.; et al. Centrifugal Microfluidics for Cell Analysis. *Curr. Opin. Chem. Biol*. **2012**, *16*, 409–414.

16. Ducrée, J.; Haeberle, S.; Lutz, S.; et al. The Centrifugal Microfluidic Bio-Disk Platform. *J. Micromech. Microeng*. **2007**, *17*, S103–S115.

17. Kirby, D.; Siegrist, J.; Kijanka, G.; et al. Centrifugo-magnetophoretic Particle Separation. *Microfluid. Nanofluid*. **2012**, *16*, 1–10.

18. Boettcher, M.; Jaeger, M. S.; Riegger, L.; et al. In *In Lab-on-Chip-Based Cell Separation by Combining Dielectrophoresis and Centrifugation;* Paper presented at the conference on Bio-Systems; 2006; Vol. 1, pp 443–451.

19. Pamme, N.; Wilhelm, C. Continuous Sorting of Magnetic Cells via On-Chip Free-Flow Magnetophoresis. *Lab Chip* **2006**, *6*, 974–980.

20. Mach, A. J.; Kim, J. H.; Arshi, A.; et al. Automated Cellular Sample Preparation Using a Centrifuge-on-a-Chip. *Lab Chip* **2011**, *11*, 2827–2834.

21. Panaro, N. J.; Lou, X. J.; Fortina, P.; et al. Micropillar Array Chip for Integrated White Blood Cell Isolation and PCR. *Biomol. Eng*. **2005**, *21*, 157–162.

22. Steigert, J.; Haeberle, S.; Brenner, T.; et al. Rapid Prototyping of Microfluidic Chips in COC. *J. Micromech. Microeng*. **2007**, *17*, 333–341.

23. Hosokawa, K.; Sato, K.; Ichikawa, N.; et al. Power-free Poly(dimethylsiloxane) Microfluidic Devices for Gold Nanoparticle-Based DNA Analysis. *Lab Chip* **2004**, *4*, 181–185.

24. Meeker, D. Finite Element Method Magnets. In *Finite Element Method Magnetics*, 4.2.

25. Rasband, W. *ImageJ*. National Institutes of Health: Bethesda, MA, 1997–2012.

26. Watkins, N. N.; Sridhar, S.; Cheng, X.; et al. A Microfabricated Electrical Differential Counter for the Selective Enumeration of CD4+ T Lymphocytes. *Lab Chip* **2011**, *11*, 1437–1447.

27. Burger, R.; Reith, P.; Kijanka, G.; et al. Array-Based Capture, Distribution, Counting and Multiplexed Assaying of Beads on a Centrifugal Microfluidic Platform. *Lab Chip* **2012**, *12*, 1289–1295.

28. Steigert, J.; Brenner, T.; Grumann, M.; et al. Integrated Siphon-Based Metering and Sedimentation of Whole Blood on a Hydrophilic Lab-on-a-Disk. *Biomed. Microdevices* **2007**, *9*, 675–679.

29. Riegger, L.; Grumann, M.; Steigert, J.; et al. Single-Step Centrifugal Hematocrit Determination on a 10-\$ Processing Device. *Biomed. Microdevices* **2007**, *9*, 795–799.

30. Haeberle, S.; Brenner, T.; Zengerle, R.; et al. Centrifugal Extraction of Plasma from Whole Blood on a Rotating Disk. *Lab Chip* **2006**, *6*, 776–781.

31. Jensen, B. N.; Lisse, I. M.; Gerstoft, J.; et al. Cellular Profiles in Bronchoalveolar Lavage Fluid of HIV-Infected Patients with Pulmonary Symptoms: Relation to Diagnosis and Prognosis. *AIDS* **1991**, *5*, 527–534.

32. World Health Organization. Technical Brief on CD4 Technologies. World Health Organization: Geneva, Switzerland, **2010**.

33. Haferlach, T.; Kohlmann, A.; Schnittger, S.; et al. Global Approach to the Diagnosis of Leukemia Using Gene Expression Profiling. *Blood* **2005**, *106*, 1189–1198.

34. Deman, J. J.; Bruyneel, E. A.; Mareel, M. M. A Study on the Mechanism of Intercellular Adhesion. *J. Cell Biol*. **1974**, *60*, 641–652.

35. Grundy, C. L.; Medina Lara, A.; Winogron, D.; et al. Point-of-Care CD4 Tests Can Increase Life-Years Saved with Reduced Costs Compared to Flow Cytometric CD4 Counting. *Sixth International AIDS Society Conference on HIV Pathogenesis, Treatment and Prevention*; **2011**, Abstract MOAD0105.